Food Chemistry: X 24 (2024) 101829

Contents lists available at ScienceDirect

Food Chemistry: X

journal homepage: www.sciencedirect.com/journal/food-chemistry-x

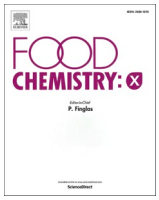

In vivo absorption, *in vitro* digestion, and fecal fermentation properties of non-starch polysaccharides from Chinese chestnut kernels and their effects on human gut microbiota

Fei Peng [a,b,1], Zuoqing Yu [a,1], Kui Niu [a,b], Bin Du [a,b], Shujun Wang [c,**], Yuedong Yang [a,b,*]

[a] Hebei Key Laboratory Of Active Components and Functions In Natural Products, Hebei Normal University of Science and Technology, Qinhuangdao 066000, China
[b] Engineering Research Center of Chestnut Industry Technology, Ministry of Education, Qinhuangdao 066000, China
[c] State Key Laboratory of Food Nutrition and Safety, Tianjin University of Science & Technology, Tianjin 300457, China

ARTICLE INFO

Keywords:
Non-starch polysaccharides
Chestnut kernels
Digestion
Fermentation
Gut microbiota

ABSTRACT

Non-starch polysaccharides are major bioactive components in chestnuts, and can serve as water-soluble polysaccharides with potential prebiotic properties. This study aims to establish an *in vitro* digestion and fermentation model to reveal the digestive and fermentative characteristics of Non-starch polysaccharides from chestnut kernels (NSPCK). The results indicated that under simulated digestion, NSPCK was partially digested in gastric juice but remained significantly undigested in saliva and intestinal juice, demonstrating considerable resilience against hydrolysis. After digestion, NSPCK still exhibited stable rough, lamellar, and porous structure and maintained strong antioxidant capacity. Animal experiments revealed positive effects of NSPCK on blood lipid level, and colon tissue of mice. Moreover, NSPCK enhanced the accumulation of short-chain fatty acids during fermentation, particularly acetic acid, propionic acid, and butyric acid. Furthermore, NSPCK intervention increased the abundance of beneficial bacteria such as *Lactobacillus* and *Bifidobacterium*, and at the same time reduced that of harmful bacteria such as *Enterococcus*.

1. Introduction

Non-starch polysaccharides (NSP) are composed of complex carbohydrate structures that exclude starch, and their formation involves the glycosidic bond linkage of ten or more monosaccharide units. These polysaccharides are predominantly constituted by substances such as cellulose, hemicellulose, pectin, fructan, mannan, and galactomannan, among other constituents (Uthumporn et al., 2017). Numerous studies have indicated that naturally sourced NSP are a category of compounds closely associated with the health status of organisms and characterized by a variety of biological functionalities (L. Wang et al., 2015; Y. Zhang et al., 2024). Notably, the biological activity of polysaccharides is intricately linked to their molecular weight, monosaccharide composition, glycosidic bond type, and modulation of gut microbiota. Specifically, polysaccharides have the potential to regulate intestinal flora, stimulate the production of short-chain fatty acids (SCFAs), and enhance the integrity of the intestinal mucosal barrier. (Xue et al., 2024). Due to their inherent properties of high molecular weights, intricate molecular architectures, and unique glycosidic bond linkages, NSP are resistant to digestion in human gastrointestinal system and then transported to the colon for fermentation to produce SCFAs, which will provide energy for probiotics and promote the growth of *Bifidobacterium* and *Lactobacillus* (Ge et al., 2024). Additionally, NSPs can lower colonic pH through microbial fermentation, thereby inhibiting the growth of certain potentially pathogenic microorganisms such as *Ruminococcus*, *Coprococcus*, and *pneumococcus* (Chen et al., 2022). Polysaccharides degraded by intestinal flora not only serve as an energy source and nutrition for host large intestine cells and other intestinal epithelial cells but also generate metabolites like short-chain fatty acids that reduce metabolic endotoxin levels, downregulate the expression of inflammatory factors, and

* Corresponding author at Hebei Key Laboratory Of Active Components and Functions In Natural Products, Hebei Normal University of Science and Technology, Qinhuangdao 066000, China.
** Corresponding author.
E-mail addresses: yuedongyang@hotmail.com, yyd1769@hevttc.edu.cn (Y. Yang).
[1] These authors contributed equally.

https://doi.org/10.1016/j.fochx.2024.101829
Received 28 May 2024; Received in revised form 4 September 2024; Accepted 9 September 2024
Available online 18 September 2024

enhance intestinal mucosal immune function (Wijesekara et al., 2024).

Nevertheless, before polysaccharides can exert their prebiotic functions upon entering the intestine, they have to pass through the oral cavity and the gastrointestinal digestive apparatus, a journey during which they may undergo changes in structure and characteristics under the action of diverse metabolic enzymes and exposure to acidic environments within the digestive system. To delve deeper into the effects of polysaccharide structures on host well-being and meticulously trace the intricate digestive progression of polysaccharides within the human gastrointestinal pathway, *in vitro* digestion models have become a robust substitute for *in vivo* digestion models. These models are characterized by merits including reduced costs, abbreviated timelines, simplified procedures, and enhanced amenability to replication and manipulation (Egger et al., 2019).

In China, chestnuts have been traditionally acclaimed as "the King of Dried Fruits" due to their extremely rich nutrients, notable health-promoting effects, and substantial pharmacological value. NSP have been identified as a key set of bioactive constituents in chestnuts, demonstrating an array of physiological functionalities, such as antioxidant, fatigue-resisting, tumoricidal, and immunity-enhancing properties (Li et al., 2022). Polysaccharides may undergo variations in their molecular weight, chemical constitution, structure, and configuration with the changes in pH level, the presence of bile salts, and the action of digestive enzymes within the gastrointestinal digestive environment, thereby showing changes in their biological activities (Geng et al., 2023). The nutritional and health benefits of chestnut polysaccharides are closely associated with their digestion, absorption, and fermentation properties within the gastrointestinal tract. However, there has been a significant dearth of fundamental research and data concerning the NSP in chestnuts, which hinders a comprehensive understanding of their nutritional and health attributes and impedes the development of high-quality nutraceutical products from chestnuts. Therefore, the objective of this study was to investigate the structural and physiological changes in chestnut polysaccharides during *in vitro* digestion simulation. Additionally, we assessed the impact of non-starch polysaccharides from chestnut kernels (NSPCK) on short-chain fatty acid (SCFA) production and gut microbiota composition to unveil its prebiotic potential. This discovery may serve as a basis for enhancing and expanding our understanding of the prebiotic properties of chestnut polysaccharides, while also offering novel insights into the structure and health benefits of dietary polysaccharides from diverse sources.

2. Materials and methods

2.1. Materials and reagents

Fresh chestnuts were purchased from the local market in Qinhuangdao City (Hebei Province, China). α-amylase (Art. No.: S27229; 40,000 U/g) and saccharifying enzyme (Art. No.: S10017; 100,000 U/g) were obtained from Shanghai Yuanye Biotechnology Co., Ltd. Neutral protease (Art. No.: RM1011; 50 U/mg) was provided by Ruiyong Biological Co., Ltd. Hydrochloric acid and sodium hydroxide of analysis purity were purchased from Tianjin Fengchuan Chemical Reagent Technology Co., Ltd. Anhydrous ethanol of analysis purity was obtained from Shanghai Titan Chemical Co., Ltd. Artificial gastric juice (Art. No.: R30387) and artificial small intestine juice (Art. No.: R30384) were provided by Shanghai Yuanye Biotechnology Co., Ltd.

2.2. Preparation of NSPCK

NSPCK was prepared with the enzymatic-alkaline method. Briefly, the initial step involved that the addition of 11 % mixed enzymes (α-amylase: glucoamylase, 4: 1) were added to the NSPCK solution (1:20 g/mL, pH = 6.3) for extraction at 60 °C for 60 min. Subsequently, 4 % neutral protease was introduced for extraction, with the temperature and time set at 60 °C and 75 min, respectively. Thereafter, NSPCK extraction was proceeded at 50 °C for 60 min at a constant pH of 9. Concurrently, deproteinized by the Sevage method, and the supernatant underwent dialysis using ultrapure water (3500 Da molecular retention), followed by ethanol precipitation and subsequent freeze-drying (Alpha 2–4 L Dplus freeze-drying machine, CHRIST, Germany).

2.3. In vitro digestion of NSPCK

Simulated saliva and gastrointestinal digestion processes were conducted based on the modified method described by Geng (Geng et al., 2023; Song et al., 2023). The prepared NSPCK solution was mixed with artificial saliva (30.0 ml) at pH 6.8, and the mixture was incubated at 37 °C. The sample (2 mL) was digested at different time points and the enzyme was inactivated in boiling water bath. The saliva mixture residue was mixed with artificial gastric juice (30.0 mL), and the pH was adjusted to 2.0. Digestion samples (2 mL) were collected at different time points and enzyme was inactivated. The simulated intestinal digestion process involved mixing the gastric digestion residue with artificial intestinal juice at a ratio of 1: 15 g/mL, maintaining a pH of 7.5, and incubating at 37 °C. Similarly, samples were collected at different time points and enzyme inactivation was performed.

Components for simulated saliva: H_2O (1 L), NaCl (0.35 g/L), KCl (0.4 g/L), $CaCl_2$ $2H_2O$ (0.1 g/L), $NaHCO_3$ (0.5 g/L), Na_2HPO_4 (0.2 g/L), amylase (0.03 g/L) were used. Components for simulated gastric juice: after adjusting the pH of H_2O (1 L) to 2 with HCl (1 mol/L), 3 g/L of pepsin was added. Then, NaCl (94.4 mmol/L), $NaHCO_3$ (50 mmol/L), KCl (13.8 mmol/L), KH_2PO_4 (1.8 mmol/L), $(NH_4)_2CO_3$ (1 mmol/L), $CaCl_2$ $2H_2O$ (0.3 mmol/L), and $MgCl_2$ $6H_2O$ (0.24 mmol/L) were used. Components for simulated intestinal juice: H_2O (1 L), NaCl (6.8 g/L), KCl (0.3 g/L), $CaCl_2$ $2H_2O$ (0.35 g/L), $NaHCO_3$ (10 g/L), Pancreatic enzyme mixture (1 g/L) were used.

The reducing sugar content was determined using the 3,5-dinitrosalicylic acid method, and the determination of total sugar content is carried out using the phenol sulfuric acid method (SPECTRA MAX 190 ELISA reader, Shanghai Meigu Molecular Instruments, Co., Ltd. China). The hydrolysis degree of the sample was calculated according to Formula (1).

$$\text{Hydrolysis}\ (\%) = \text{Reducing sugar}/(\text{Total sugar} - \text{Initial reducing sugar}) \times 100\% \quad (1)$$

Among them, hydrolyzed reducing sugar was calculated as the difference between the mass of reducing sugar measured at a certain time point and the initial mass of reducing sugar (mg).

2.3.1. Chemical composition

By adopting the method of Geng et al. (Geng et al., 2023), the digestibility of NSPCK was calculated, and the total polysaccharides, proteins, and reducing sugar contents of NSPCK and their digested samples were measured by the phenol-sulfuric acid method, Coomassie brilliant blue method, and DNS method, respectively.

2.3.2. Structural analysis

The surface structure of NSPCK was determined using scanning electron microscope (Hitachi Corporation, Japan). The molecular weight (Mw) of NSPCK was determined using high-performance liquid chromatography (HPLC1100, Agilent, USA). The monosaccharide composition was determined using high-performance anion exchange chromatography equipped with amperometric detection (ICS5000+, Thermo Fisher Scientific, USA). NSPCK samples were conducted infrared spectroscopy analysis (TENSOR27, Fourier Transform Infrared Spectrometer Bruker, Germany). The particle size was determined by preparing 1 % NSPCK samples of pre- and post- digestion, dissolving them in distilled water, and then directly measuring them using a BT-90 nm laser particle size distribution instrument (Dandong Baite Instrument Co., Ltd., China) (Geng et al., 2023).

2.3.3. Bioactivity analysis

The antioxidant activities (DPPH, ABTS, T-AOC radical-scavenging capacities) of NSPCK and digested samples were determined with related test kits (Solarbio Science, Beijing, China). Moreover, enzyme inhibitory activities (α-glucosidase, α-amylase) of NSPCK and digested samples were determined by published methods (Juśkiewicz et al., 2023).

2.4. Animal experiments

The experiments were conducted in strict accordance with the National Institute of Health guidelines, and were approved by the Animal Ethics Committee of Hebei Normal University of Science and Technology, and analysis and Testing Research Center. Thirty SPF-grade, six-week-old male C57BL/6 mice were acclimated through adaptive feeding for one week. They were then randomly and equally divided into three groups ($n = 10$):the blank group (CK), low dose NSPCK (NSPCK-L) and high dose NSPCK (NSPCK-H). Each mouse in NSPCK-L and NSPCK-H was orally administered 100 mg/kg BW and 200 mg/kg BW of NSPCK, respectively, while the CK group received the same amount of normal saline. The experiment lasted for four weeks, during which all animals enjoyed free access to water and feed. The body weights and fasting blood glucose levels were recorded weekly.

2.5. Biochemical index and histological analysis

Upon the end of experiments, euthanasia of mice was carried out *via* cervical dislocation. Blood was collected *via* retro-orbital bleeding, followed by serum isolation for automated biochemical analysis to determine the levels of total cholesterol (TC), triglycerides (TG), high-density lipoprotein (HDL—C), and low-density lipoprotein (LDL-C). Hepatic and other tissues were collected from the mice, immersed in a 4 % neutral buffered formaldehyde solution for histological processing and hematoxylin-eosin (H&E) staining.

2.6. In vitro fermentation of NSPCK

2.6.1. Simulated fermentation process

The *in vitro* fermentation of the NSPCK was performed by using a previously described method (Geng et al., 2023). Fresh fecal samples were collected from four individuals, comprising two males and two females aged between 19 and 24 years, who had abstained from consuming relevant antibiotics within the preceding three months. The feces were thoroughly mixed with PBS (30 % *w/v*) and subsequently filtered through sterile gauze. A 9 mL aliquot of the basal nutrient solution containing varying concentrations of samples was mixed with 1.0 mL of 10 % fecal slurry, followed by incubation in an anaerobic atmosphere (10 % H_2, 10 % CO_2, and 80 % N_2) within a constant temperature shaker at 37 °C and 200 rpm (Y—O_2 Anaerobic incubator, Shanghai Binglin Electronic Technology Co., Ltd., China). According to the experimental requirements, the fertilization products were collected at different time points for analysis. The basic medium included 10 g/L protein peptone, 3 g/L soy peptone, peptone 10 g/L, 13.5 g/L serum digestion powder, 2.2 g/L beef soaking powder, 5 g/L yeast soaking powder, 3 g/L glucose, 1.2 g/L beef liver soaking powder, 3 g/L sodium chloride, 5 g/L soluble starch, 2.5 g/L potassium dihydrogen phosphate, 0.3 g/L L-cysteine, 0.3 g/L sodium thioglycolate, 5 mg/L hemin solution, and 1 mg/L vitamin K1. The original fecal suspension was taken as the control group (CK), and NSPCK was taken as the experimental group.

2.6.2. Physico-chemical properties

At different culture time points, the culture samples were taken 1.0 mL of the culture sample and centrifuge to obtain the supernatant. The pH of the supernatant, along with its OD_{600}, reducing sugar content, total sugar content, and Mw were measured.

2.6.3. SCFAs

The contents of SCFAs in fermentation samples were determined by gas chromatography (GC, Thermo Scientific, Germany), which was equipped with an HP-5MS capillary column (30 m × 0.25 mm × 0.25 μm). Other parameters were set based on a previous method with mild modification (Juśkiewicz et al., 2023). Briefly, both the injector and detector were maintained at 250 °C, and the column temperature was held constant at 100 °C for 5 min, and then increased at a speed of 4 °C/min from 100 to 180 °C for 3 min.

2.6.4. Gut microbiota analysis

After 24 h of fermentation, DNA was extracted from the fermentation mixture. The V3–V4 variable region of the 16SrRNA gene was amplified by PCR using the speciffc primers 338F (5'-ACTCCTACGGGAGGCAGCAG-3′) and 806R (5'-GGACTACHVGGGTWTCTAAT-3′). After performing PCR ampliffcation, the qualiffed libraries were sequenced using Illumina NovaSeq PE250 platform by Jiangsu SanShu Biotechnology Co., Ltd. (Nantong, China). OTU clustering was performed using UPARSE at a similarity level of 97 %. Statistical methods were used to analyze the differences in microbial community composition between sample groups and identify the microbial species with significant differences.

2.7. Statistical analysis

The data were conducted in five parallel groups, with the average value taken as the response value of NSPCK. The significance of different factors on NSPCK extraction was determined through analysis of variance. The difference between the means was considered as statistically significant at $p < 0.05$. Each experiment was performed in triplicate.

3. Results and discussion

3.1. Effect of in vitro digestion on the structural properties of the NSPCK

Cleavage of polysaccharide glycosidic bonds can increase the reducing sugar content. Hence, reducing sugar content can serve as an indicator of the degradation degree of these bonds by digestive enzymes. As shown in Fig. 1a, the initial reducing sugar contents of NSPCK upon entry into the salivary, gastric, and intestinal digestion phases were 6.133 ± 0.122 mg/mL, 6.045 ± 0.233 mg/mL, and 3.063 ± 0.055 mg/mL, respectively. In the salivary digestion phase, the reducing sugar content slightly increased to 6.155 ± 0.167 mg/mL, but the increment was not statistically significant ($p > 0.05$). After 4-h simulated *in vitro* gastric digestion, the reducing sugar content of NSPCK showed a significant increase to 6.690 ± 0.248 mg/m ($p < 0.05$). In the simulated intestinal digestion, no significant difference ($p > 0.05$) was detected in reducing sugar content of NSPCK across the time points of 0, 1, 2, 3, and 4 h. As shown in Fig. 1b, an analysis of the hydrolysis degree resulting from saliva, gastric, and small intestinal digestion revealed that throughout the salivary and intestinal digestion processes, the

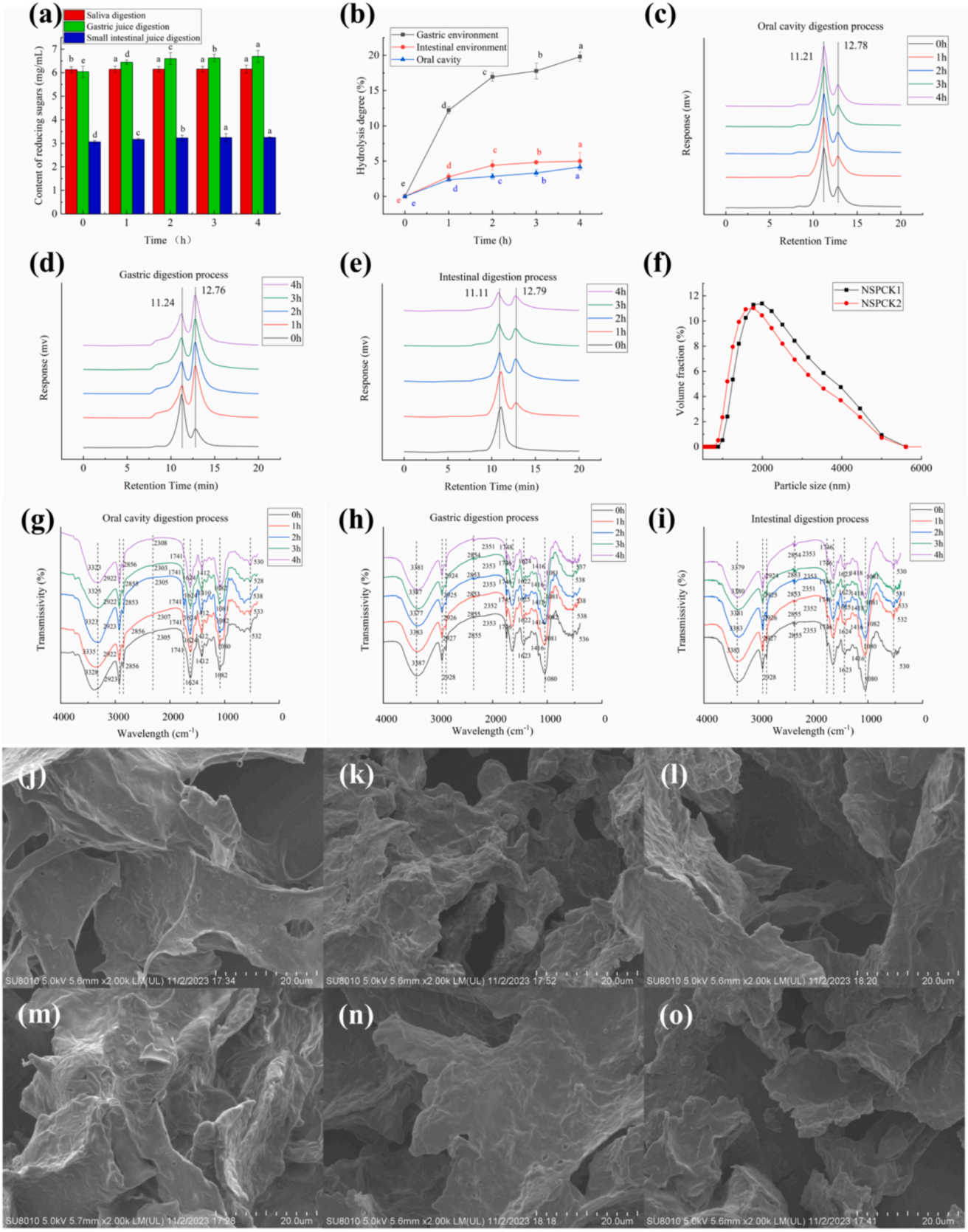

Fig. 1. Content of reducing sugars of NSPCK after simulated digestion (a). Hydrolysis degree of NSPCK in artificial saliva, gastrointestinal juice (b). Mw of NSPCK in saliva (c), gastric juice (d) and intestinal juice (e). Particle size of NSPCK in digestive juice (f). FT-IR of NSPCK in saliva (g), gastric juice (h) and intestinal juice (i). SEM of NSPCK in pre- (j-l) and post- (m-o) digestive juice. Enlargement at 2000× in saliva (j, m), gastric juice (*k*,n), and small intestine juice (l, o). Different superscript lowercase letters indicate significant differences ($p < 0.05$).

Table 1
The MW of NSPCK samples was analyzed at various time points.

Name	Simulate saliva environment		Simulate gastric environment		Simulate intestinal environment	
Mw (kDa)	M_n	M_w	M_n	M_w	M_n	M_w
0 h	8505	11,319	8575	11,395	11	101
1 h	8511	11,332	13	937	11	155
2 h	8528	11,346	14	975	15	487
3 h	8524	11,342	15	988	17	690
4 h	8533	11,356	15	986	18	743

M_n: number-average molecular weight, M_w: weight average molecular weight.

hydrolysis degree of NSPCK was consistently maintained below 5 %, indicating insignificant digestion of NSPCK in both the oral cavity and the intestine ($p < 0.05$) (Riyadi et al., 2023). The maximum hydrolysis degree was observed after 4 h of digestion in each phase, with the values being recorded as 4.17 ± 0.42 % in the salivary phase, 19.80 ± 0.70 % in the gastric phase, and 4.99 ± 1.23 % in the intestinal phase.

Changes in the Mw of NSPCK during salivary and gastrointestinal digestion are depicted in Fig. 1c-e and Table 1. After digestion under simulated gastric conditions, the Mw showed a marked decline from 0 to 1 h, while no significant change between 1 and 4 h, suggesting partial digestion of NSPCK in the gastric environment. In contrast, during the simulated salivary and small intestinal digestion, the Mw exhibited a consistent and gradual but statistically not significant increase.

As the first site of digestion after food intake, the oral cavity secretes salivary α-amylase to specifically cleave α-1,4-glycosidic bonds, which is capable of breaking down most soluble digestible starches. In this study, NSPCK remained nearly undigested after simulated salivary digestion (Fig. 1b), suggesting the absence of α-1,4-glycosidic linkages in NSPCK. Notably, most naturally occurring non-starch polysaccharides from plants are indigestible by human saliva. During simulated gastric digestion, NSPCK experienced a marked increase in reducing sugar content along with a decrease in Mw (Fig. 1a and Tables 1), implying that NSPCK can stably persist in the oral cavity, stomach, and intestine, with partial digestion occurring in the gastric environment. This may be attributed to the acidic pH, bile salts, and digestive enzymes involved in gastric digestion (Luo et al., 2023), which is consistent with our results. Furthermore, the small intestinal digestive juice showed a minimal impact on NSPCK, indicating that NSPCK has a higher stability in the intestinal environment than in the gastric environment. Fig. 1a and Table 2 reveal that the rise in pH was correlated with the decline in hydrolysis degree, primarily due to the accelerated leaching of glucose components from NSPCK under acidic conditions, which reduces polymerization and thereby enhances hydrolysis. Conversely, NSPCK demonstrated strong resistance to α-amylase hydrolysis under weakly alkaline conditions (W. Zhang et al., 2017).

Table 2
Changes in components of NSPCK during digestion.

Components	NSPCK (%)	NSPCK-S (%)	NSPCK-G (%)	NSPCK-I (%)
Digestibility	–	0.73 ± 0.03^{c}	9.94 ± 0.12^{b}	11.27 ± 0.18^{a}
Total polysaccharide	92.08 ± 3.14^{a}	91.96 ± 2.88^{b}	84.54 ± 3.59^{c}	84.33 ± 2.11^{c}
Total proteins	1.44 ± 0.12^{a}	1.36 ± 0.45^{b}	0.95 ± 1.38^{c}	0.98 ± 0.23^{c}
Total ash	7.39 ± 0.34^{a}	7.34 ± 1.07^{b}	7.26 ± 0.11^{c}	7.25 ± 0.03^{c}
Total phenol	0.0038 ± 0.06^{c}	0.0042 ± 0.04^{a}	0.0039 ± 0.01^{b}	0.0040 ± 0.01^{b}
Constituent monosaccharides and molar ratios				
Rha	0.0263	0.0315	0.0342	0.0385
Ara	0.1174	0.1550	0.1578	0.1778
Gal	0.1447	0.2392	0.2903	0.2967
Glc	0.6121	0.4222	0.3487	0.3195
Xyl	0.0560	0.0797	0.1257	0.1289
Gal-UA	0.0156	0.0273	0.0401	0.0460

NSPCK-S denotes NSPCK subjected to salivary digestion, NSPCK-G to gastric digestion, and NSPCK-I to intestinal digestion. Values represent mean ± standard deviation. Different superscript lowercase letters indicated significance ($p < 0.05$) in each row.

It has been demonstrated that the particle size of polysaccharides influences their physicochemical properties, and its decrease tends to increase the specific surface area, thereby improving the physical and chemical properties of polysaccharides (Ding, 2021). As shown in Fig. 1f, the particle size of NSPCK primarily fell within the range of 1000–400 nm (NSPCK1). After the simulated digestion process (NSPCK2), the particle size showed a significant decrease ($p < 0.05$).

Fig. 1g-i depict the FT-IR variations of NSPCK in the stomach and intestines, which spanned the experimental time of 0–4 h. After simulated gastric digestion, the FT-IR of each NSPCK exhibited typical absorption peaks of polysaccharides. Upon simulated gastric and small intestinal digestion, the primary characteristic absorption peaks remained largely unchanged, implying that there were no substantial compositional variations. The absorption peaks included the broad bands at 3380 and 2925 cm^{-1}, which are caused by the O—H bond and C—H stretching vibration produced by hemicellulose and cellulose, and might also include the N—H stretching vibration. The O—H bond may be caused by the hydrogen bond in the uronic acid molecule, which represents the typical structure of polysaccharides (Jia et al., 2020; Sun et al., 2020). The absorption peak at 1250 cm^{-1} may be the vibration of O—H or C—O groups in hemicellulose, and the absorption peak at 1040 cm^{-1} is the stretching vibration peak of C—O on C-O-C bond, which is a typical absorption peak of xylan, indicating that NSPCK contains xylan hemicellulose (Esteves et al., 2013). The absorption peak at 1420 cm^{-1} may be assigned to the bending vibration of aliphatic or aromatic lignin C—H in NSPCK, and that at 850 cm^{-1} may be caused by the fracture of β-pyran ring, indicating that the glycosidic bond in NSPCK is mainly of a β-configuration (Xie et al., 2018). The absorption peaks near 1745 and 1620 cm^{-1} are C═O characteristic absorption peaks of carboxyl or aldehyde groups, indicating that the extracted NSPCK contains uronic acid. There was a narrow and strong absorption peak at 1033 cm^{-1}, which may be related to the stretching vibration of C-O-C bond of glucopyranoside (Hashemifesharaki et al., 2020).

SEM is the most direct tool to elucidate the complex structure of NSPCK as illustrated in Fig. 1j-o. Prior to digestion, the surface of NSPCK exhibited a rough texture characterized by compact stacking of ordered lamellar and porous structures. Notably, no significant change was observed in surface morphology after the digestion process.

Table 2 summarizes the changes in chemical composition and digestibility of NSPCK during the digestion process. After salivary, gastric, and intestinal digestion, the digestibility of NSPCK was 0.73 ± 0.03 %, 9.94 ± 0.12 %, and 11.27 ± 0.18 %, respectively, indicating its partial breakdown by gastric juice. Moreover, NSPCK initially comprised 92.08 ± 3.14 % polysaccharides, 1.44 ± 0.12 % proteins, and 0.0038 ± 0.06 % phenols, while the levels of polysaccharides and proteins decreased to 84.33 ± 2.11 % and 0.98 ± 0.23 % after digestion, respectively. Other components showed insignificant changes ($p > 0.05$).

In terms of monosaccharide composition (Table 2), NSPCK primarily consisted of rhamnose, arabinose, galactose, glucose, xylose, and galacturonic acid. After digestion, the molar ratio of glucose decreased from 0.6121 to 0.3195, leading to a proportional increase in the molar ratio of other monosaccharides, which suggested that glucose is primarily consumed during gastrointestinal digestion, particularly in the gastric phase, and its release increases the reducing sugar content and therefore promotes the hydrolysis degree in gastric juice (Li, Zhou, et al., 2022). No marked differences ($p > 0.05$) were observed for other monosaccharides except for glucose. Collectively, it can be inferred that NSPCK primarily undergoes a decrease in polymerization degree during digestion without glycosidic bond rupture or structural modification. Hence, it can be further speculated that NSPCK may be commendably metabolized by colonic and cecal gut microbiota.

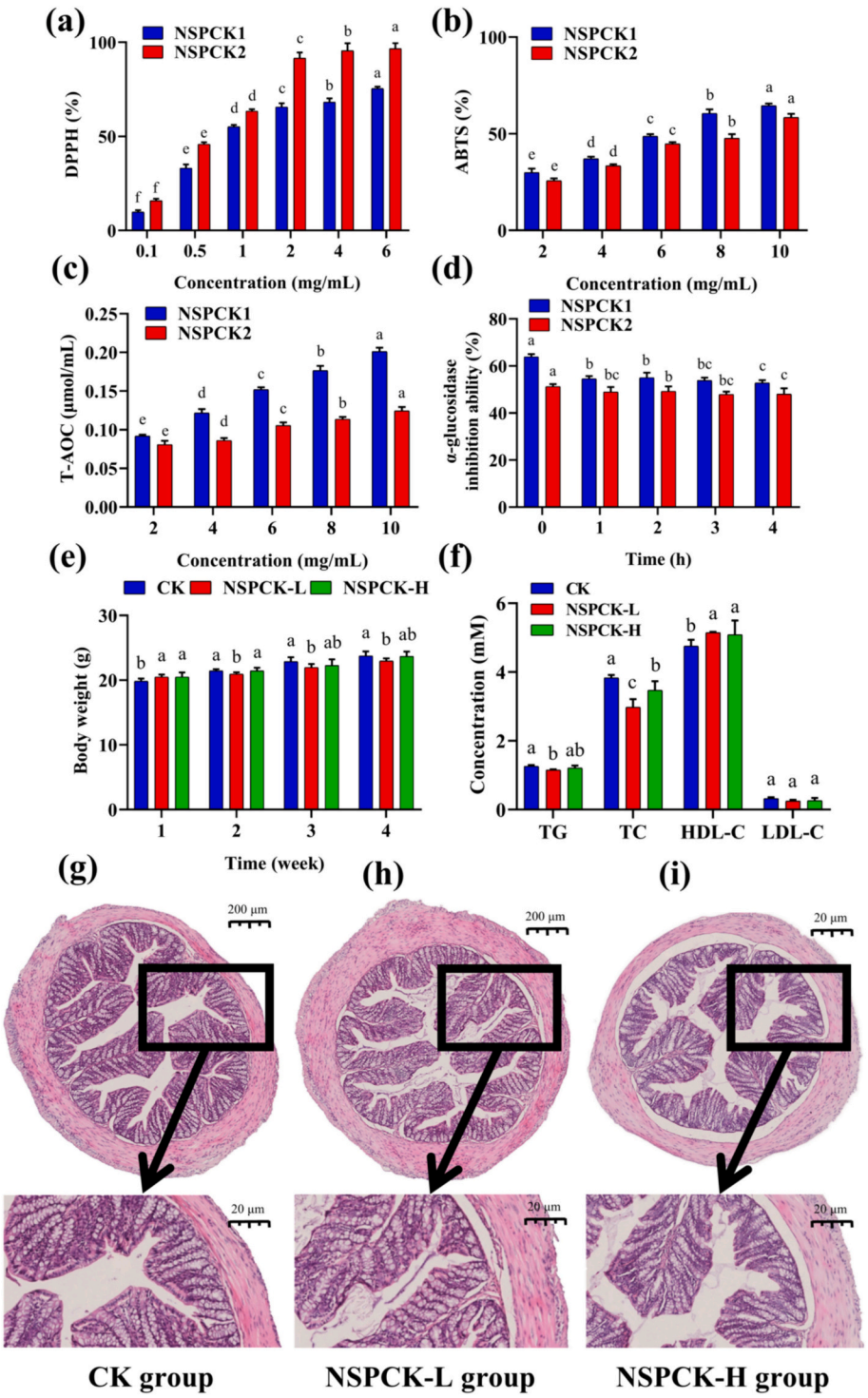

Fig. 2. Changes in biological activities of NSPCK during *in vitro* digestion. DPPH (a), ABTS (b) and T-AOC (c), respectively, pre- (NSPCK1) and post- (NSPCK2) digestion; α-glucosidase inhibition capacity (d) of NSPCK, in gastric (−G) and intestinal (-I) juice. Effects of NSPCK-L (low dose NSPCK) and NSPCK-H (high dose NSPCK) on body weight (e), blood lipid level (f) and colon tissue (g-i) in diabetes mice, compared with the CK group. Data are expressed as mean ± standard deviation ($n = 3$). Different letters (a, b, c, d, e) indicate significant differences between groups ($p < 0.05$).

3.2. Effect of in vitro digestion on the antioxidant and hypoglycemic activity of NSPCK

Fig. 2a-c show that NSPCK exhibits concentration-dependent relationships with DPPH, ABTS, and T-AOC, respectively. After digestion, the ability of NSPCK to scavenge DPPH radicals was significantly improved, with the value rising from 75.49 ± 0.01 % to 96.59 ± 0.03 % at the concentration of 6 mg/mL. Conversely, the antioxidant activities against ABTS and T-AOC decreased from 64.55 ± 1.07 % to 58.48 ± 1.82 % and from 20.12 ± 0.01 % to 12.45 ± 0.01 % at the concentration of 10 mg/mL, respectively.

As illustrated in Fig. 2d, the α-glucosidase inhibition experiment revealed that NSPCK has a strong inhibitory effect on α-glucosidase with an inhibition rate of 63.79 ± 2.11 %. After simulated salivary, gastric,

and intestinal digestion, the α-glucosidase inhibition capability of NSPCK significantly declined to 48.07 ± 2.52 %, particularly after 1 h of gastric digestion when the inhibition capability dropped to 54.57 ± 1.10 % ($p < 0.05$).

Generally, the Mw and monosaccharide composition of natural polysaccharides play a pivotal role in their antioxidant properties. Our data illustrated that digestion significantly elevates the DPPH value while decreases the ABTS, T-AOC, and α-glucosidase inhibitory ability; however, NSPCK retained considerable physiological activity after digestion, indicating its enduring bioactive potential even after digestion (Fig. 2a-d). These results might be associated with the observed decreases in Mw and particle size in Table 1 and Fig. 1e. It has been demonstrated that the inhibitory effect of polysaccharides on the *in vivo* glucose-lowering enzyme activity is closely related to their chemical structure (Geng et al., 2023). Hence, the decreases in α-glucosidase inhibitory activity of NSPCK and its digestion products after simulated *in vitro* digestion may be associated with Mw reduction and conformational changes induced by the digestive environment.

3.3. Effect of NSPCK on the body weight, blood lipid levels and colon tissue in mice

Fig. 2e illustrates that both the CK and NSPCK groups showed steady increases in body weight over time, with the overall body weight of the NSPCK group being no significantly changes than that of the CK group ($p > 0.05$). Moreover, compared with the CK group, either the low or high dose in NSPCK group (Fig. 2f) showed a significant reduction in serum TG and TC levels ($p < 0.05$), while a notable increase in the HDL-C level ($p < 0.05$); however, no significant difference in LDL-C level was observed ($p > 0.05$). H&E staining results (Fig. 2g-i) revealed that NSPCK-L and NSPCK-H group had no apparent pathological changes in colon tissue compared with the CK group, suggesting that NSPCK causes no damage to the colon tissue of mice. On the contrary, NSPCK was found to increase the thickness of the mucosal and muscular layers in mice, exhibiting a positive effect on the intestinal barrier function of mice. The results of our study suggest that a daily intake of NSPCK not exceeding 200 mg/kg has a beneficial impact on both lipid levels and colon tissue in mice, while having no significant effect on body weight.

3.4. Effects of in vitro fecal fermentation on NSPCK

The data demonstrated that NSPCK could resist gastrointestinal digestion, and is therefore able to reach the colon, where it can interact with the gut microbiota. During the fermentation process, the fermentation broth showed obvious changes in total sugars and reducing sugars (Fig. 3a-b). In the first 4 h of fermentation, the contents of both total sugars and reducing sugar showed a rapid increase, followed by a declining trend.

pH is a pivotal indicator of organic acid production by gut microbiota. Here, the pH exhibited a marked decline in the fermentation broth of the NSPCK group over 48 h of fermentation as shown in Fig. 3c, with the value ranging from 6.54 to 4.03 ($p < 0.05$). At the onset of fermentation (0 h), no statistically significant difference in pH was detected between the NSPCK group and the CK group ($p > 0.05$). However, there was a significant difference in pH after 48 h of fermentation between the two groups ($p < 0.05$).

In the *in vitro* fermentation experiment, changes in the OD_{600} value could reflect the growth of microbes in the fermentation broth (Geng et al., 2023). As depicted in Fig. 3d, after 6 h of fermentation, the OD_{600} value for both the CK and NSPCK groups reached the peak of 0.155 and 0.253, respectively, implying rapid bacterial proliferation. From 6 to 48 h, the OD_{600} showed a generally decreasing trend, indicating a decline in bacterial population over time.

Previous studies have indicated that gut microbiota can harness indigestible polysaccharides by the human body. The fermentation rate of polysaccharides by gut microbiota is found to be contingent upon their physicochemical characteristics and structure. *In vitro* fermentation assays in this study demonstrated that NSPCK can effectively lower the intestinal pH and facilitate the proliferation of gut microbiota, and the changing trend is possibly associated with varying utilization efficiency of different polysaccharides (Salvador et al., 1993). The decline in pH is associated with the production of SCFAs, and a marked alteration in the composition of microbial colonies occurred when the pH of the *in vitro* fermentation medium decreased to 5.5 (Chen, Luan, et al., 2023).

3.5. Effect of NSPCK on SCFAs levels

SCFAs are the final products of polysaccharide fermentation by specific anaerobic gut microbiota, and are primarily responsible for the reduction in pH. Fig. 3e-j illustrates the differences in SCFAs concentration between the NSPCK group and CK group across 0–48 h of fermentation. After 48 h of fermentation, both groups displayed a significant rise in total SCFAs, which increased to 80.05 ± 2.77 μg/mL for the CK group and more substantially to 113.46 ± 7.43 μg/mL for the NSPCK group ($p < 0.05$). Notably, the addition of NSPCK significantly elevated the total SCFAs compared with the CK group ($p < 0.05$).

At the end of fermentation (48 h), the primary SCFAs metabolized by the intestinal microbiota in the NSPCK group were identified as acetic acid, propionic acid, and n-butyric acid, which reached a combined concentration of 297.27 ± 3.47 μg/mL and significantly surpassed that of the CK group (275.61 ± 2.33 μg/mL) ($p < 0.05$). Interestingly, SCFAs in the CK group generally increased during the initial 0–12 h but showed a decreasing trend from 12 to 48 h. Conversely, in the NSPCK group, SCFAs demonstrated a rapid rise within the first 0–12 h, with acetic acid, i-butyric acid, and hexanoic acid subsequently exhibiting a decline from 12 to 48 h. Moreover, propionic acid, n-butyric acid, and pentanoic acid in the NSPCK group continued to increase during 12–48 h.

SCFAs, primarily acetic acid, propionic acid, and n-butyric acid, are the primary metabolic byproducts of polysaccharide fermentation and their production is significantly correlated with the content of reducing and total sugars. It has been demonstrated that SCFAs (acetic acid, propionic acid, and butyric acid) govern the development and function of virtually all types of immune cells (Golpour et al., 2023). Acetic acid, the most abundantly produced volatile acid during fermentation, not only reflects the intensity of fermentation and efficiency of substrate utilization by the inoculated microorganisms, but also serves as a precursor for butyric acid production and is a vital energy source for intestinal cells, suppressing the appetite and modulating fat absorption (Ferreira-Lazarte et al., 2019). Hence, the substantial acetic acid production observed during NSPCK fermentation in this study ascertained that NSPCK is an efficacious carbon source. Furthermore, according to our results, acetic acid metabolism by gut microbiota mainly occurred in the early phase, with a subsequent decrease in acetic acid level and an increase in butyric acid level between 24 and 48 h (Fig. 3e, g-h), which can be attributed to reduced carbon availability and utilization in the mid-to-late stages. After being produced by gut bacteria, propionic acid can be absorbed by the human body into the bloodstream and then transported to the liver, which then downregulates the synthesis of fatty acids in the liver and plasma, inhibits immune overactivation, and increases insulin sensitivity (Al-Lahham et al., 2010). The level of propionic acid has been found to be implicated in weight loss and improvement of insulin sensitivity in severely obese individuals, and its production is mainly due to the fermentation of glucose, mannose, and arabinose (Jonathan et al., 2012). Notably, the NSPCK group displayed a sustained and substantial increase in propionic acid concentration after 48 h of fermentation (Fig. 3f), probably due to the relatively high content of glucose and arabinose (Table 2). Butyric acid, which has been recognized for its multitude of physiological roles, can preserve the structure and functional integrity of the intestinal barrier. In addition, some studies have revealed that valeric acid inhibits the synthesis of saturated fatty acids and cholesterol (Lavelle & Sokol, 2020). Similarly,

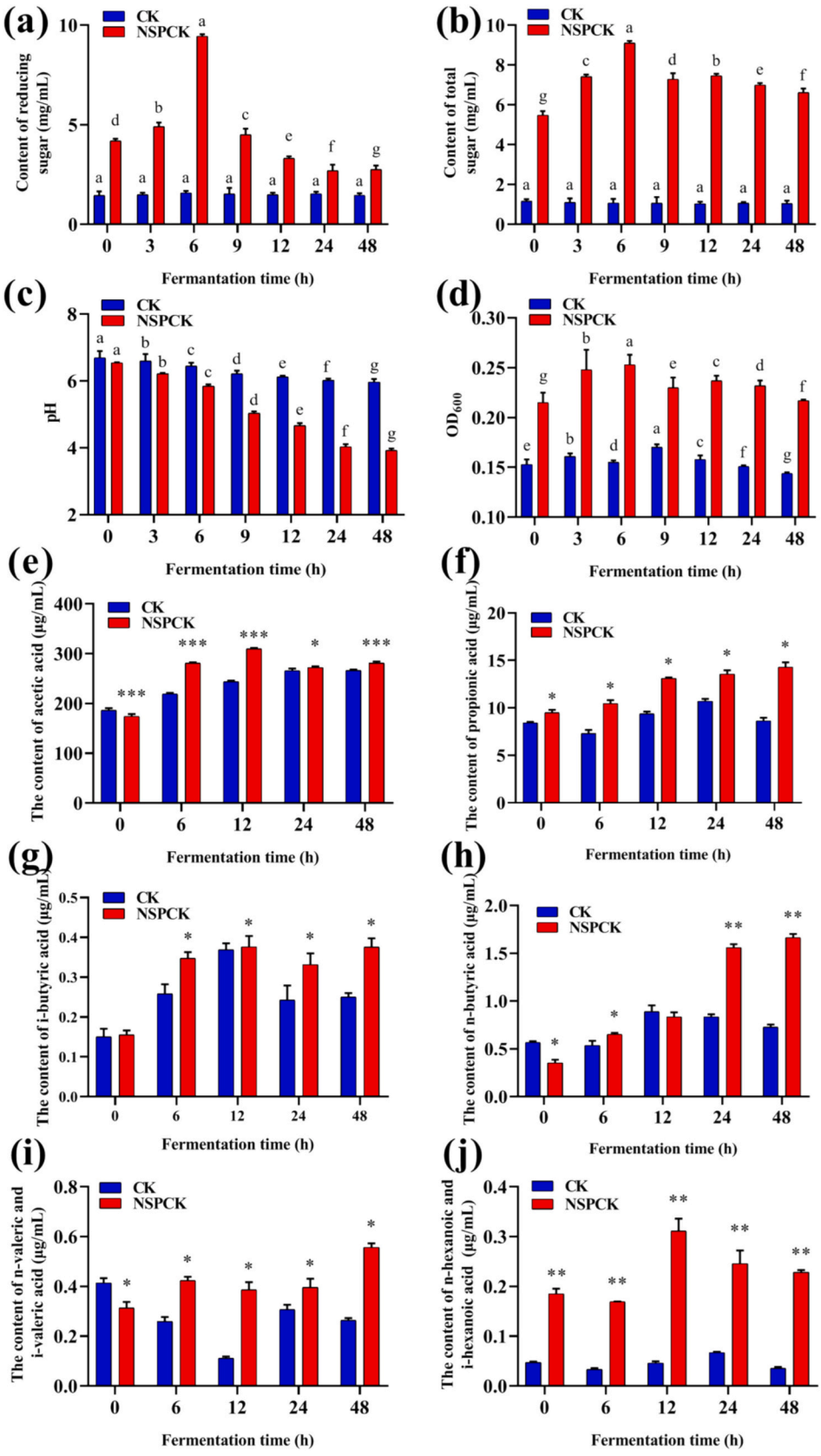

Fig. 3. Changes of *in vitro* fermentation characteristics of CK and NSPCK. Reducing sugar content (a), total sugar content (b), pH (c), OD_{600} (d). Changes in SCFAs levels in fermentation solutions (e-j). Data are expressed as mean ± standard deviation ($n = 3$), and $^{*}p < 0.05$, $^{**}p < 0.01$, $^{***}p < 0.001$. Different lowercase letters represent statistically significant differences ($p < 0.05$).

valeric and hexanoic acids have been observed to regulate some pivotal inflammatory cytokines, including IL-32 and IL-18, thereby serving as primary modulators of inflammatory responses (El-Far et al., 2021). The NSPCK group showed marked increases in valeric and hexanoic acid concentrations compared with the CK group (Fig. 3i-j). These results implied the efficient utilization of NSPCK by the gut microbiota.

3.6. Effect of NSPCK on gut microbiota

3.6.1. Effect of NSPCK on microbial species

We performed high-throughput 16S rRNA gene sequencing of fecal samples to elucidate the modulatory effects of NSPCK on the gut microbiome. The raw fecal bacterial suspension showed a normal community structure, confirming the feasibility of the collected samples for experimental manipulation. We further assessed the phylum-level composition of the microbiota in each group to investigate the impact on fecal microbial community structure (Fig. 4a). The results showed that Proteobacteria, Firmicutes, Bacteroidetes, and Actinobacteria were dominant phyla across different experimental samples. Relative to the CK group, 48 h of fermentation with NSPCK significantly increased the abundance of Firmicutes and Proteobacteria, accompanied by a decrease in that of Bacteroidetes and Actinobacteria.

To identify the specific genera involved in NSPCK metabolism, we analyzed the abundance of microbes at the genus level (Fig. 4b). As a result, intervention with NSPCK resulted in significant increases in the relative abundance of *Escherichia-Shigella*, *Bacteriodes*, *Ruminococcaceae_UCG-002*, and *Lactobacillus*, while decreased the abundance of *Dialister*, *Gammaproteobacteria_unclassified*, *Parasutterella*, *Pseudomonas*, *Enterococcus*, *Klebsiella*, and *Sutterella*. Interestingly, in the NSPCK group, the most prominent increase in abundance was noted for *Escherichia_-Shigella*, followed by *Bifidobacterium* and *Lactobacillaceae*. Moreover, the clustering tree reflected similarities in bacterial composition and highlighted the specificity of bacterial distribution. Clustering analysis of the bacterial communities demonstrated that supplementation with NSPCK greatly changed the microbiota composition (Fig. 4c), underscoring its potential in shaping the gut microbiome.

When decomposed and utilized by the gut microbiota, polysaccharides concurrently modulate the composition of the gut microbiome, thereby exerting a prebiotic effect. In this study, we found that NSPCK significantly enhanced the abundance of bacteria such as *Bifidobacterium*, *Lactobacillus*, *Ruminococcaceae UCG-002* and *Escherichia-Shigella* (Fig. 4). Wherein, the increasing abundance of *Escherichia-Shigella* in the NSPCK group may be due to the higher content of low-molecular-weight carbon sources, which may also be related to its partial hydrolysis into oligosaccharides (Chen et al., 2023; S. Chen, Liu, et al., 2023). Previous studies have shown that *Bifidobacterium* and *Lactobacillus*, among others, are capable of degrading oligofructose and polydextrose, with their abundance notably increasing after *in vitro* fermentation, indicating that beneficial gut bacteria can utilize the abundant reducing sugars in NSPCK. Notably, *Bifidobacterium*, a pivotal gut symbiont, showed remarkable changes in the gut microbiota composition of hypercholesterolemic individuals. Furthermore, the level of *Bifidobacterium* was significantly reduced in the gut of diabetic mice induced by high-fat diets (Kappel et al., 2023). The *Lactobacillaceae* family, with which humans exhibit the broadest range of positive interactions, demonstrates capability to promote growth and shield the host from pathogenic threats (Rajput et al., 2023). *Bifidobacteria*, *lactobacilli*, and other beneficial bacteria inhibit the proliferation of harmful bacteria, combat pathogenic bacterial infection, synthesize essential vitamins, facilitate mineral absorption, and produce organic acids such as acetic acid, propionic acid, butyric acid, and lactic acid, which can together stimulate intestinal motility (Kappel et al., 2023). *Ruminococcaceae UCG-002* primarily metabolizes cellulose as its carbon source, and also participates in the metabolism of proteins, lipids, and polysaccharides, releasing important metabolites such as SCFAs (H. Wang et al., 2022). NSPCK decreased the relative abundance of certain harmful bacteria. *Phascolarctobacterium*, which is prevalent in human gut microbiota, is utilized for predicting obesity indices, and individuals prone to obesity generally exhibit higher *Dialister* levels (Watanabe et al., 2012). *Parasutterella* is positively correlated with type 2 diabetes and dietary carbohydrate intake (Henneke et al., 2022). An increase in *Enterococcus* abundance is associated with higher risks of urinary tract infection, skin and soft tissue infection, life-threatening abdominal infection, sepsis, endocarditis, and meningitis (Yang, Liu, Wu, Zhu, and Liang, 2024). *Sutterella* is associated with liver fat accumulation with increased relative abundance in obese individuals (Lu et al., 2021). Collectively, after NSPCK intervention, there is a conspicuous increase in the abundance of gut microbiota involved in NSPCK metabolism and SCFAs production, coupled with a decrease in harmful bacteria, which together contribute to the potential of NSPCK to improve the gut microbiota environment.

3.6.2. Effect of NSPCK on microbial diversity

To ascertain whether NSPCK influences the microbial diversity, a further analysis of the 16S rRNA gene sequences was conducted across groups. A boxplot was used to depict the differences in operational taxonomic units (OTUs) among different groups. Fig. 5 illustrates the statistical differences in OTUs between the CK and NSPCK groups. Compared with the CK group, the NSPCK group exhibited a reduced number of species (Fig, 5a-d), and richness and diversity of microbial community (Fig. 5e-h). The two groups had a total of 89 shared species. The CK group possessed 149 unique species, while the NSPCK group had 84 unique species (Fig. 5i). PCA1 and PCA2 accounted for 30.32 % and 11 % of the variance, respectively (Fig. 5j), whereas PCoA1 and PCoA2 explained 52.94 % and 27.92 % of the variance (Fig. 5k), indicating substantial differences in reproducibility and similarity between the CK and NSPCK groups.

Previous research has shown that soluble polysaccharides contain a large amount of carbon, which is easily metabolized by gut microbiota and also limits the proliferation of many tested bacterial strains (Harris et al., 2020), and the decrease in diversity may be related to the competition between *Lactobacillus plantarum* and other bacteria, as well as the addion amount of polysaccharides. Specifically, we observed that the reduction in community abundance could be primarily attributed to a decline in pathogenic Fusobacteria, which coincides with an increase in beneficial Firmicutes. In summary, NSPCK holds considerable potential in targeted manipulation of the gut microbiota, thereby affecting the richness and diversity of the gut microbiome. This mechanism promotes the diversity and abundance of beneficial bacteria while concurrently diminishes the abundance of harmful bacteria. Hence, NSPCK plays a constructive role in facilitating the enrichment of gut microbiota.

3.6.3. LDA and LefSe

Linear discriminant analysis (LDA) is powerful in identifying significant disparities in gut microbiota under intervention, with a higher value denoting more pronounced disparity. As depicted in Fig. 6a, the LDA values fall within the range of 3–5, suggesting notable distinctions among different microbial populations (Geng et al., 2023). Linear discriminant analysis effect size (LEfSe) was employed to identify and interpret microbes with significant variations (Geng et al., 2023).

LEfSe analysis (Fig. 6b) revealed a total of three distinct taxa in the NSPCK group, including *Bifidobacteriaceae* within Actinobacteria at the genus level, *Barnesiellaceae* and *Erysipelotrichaceae* within Bacteroidetes at the family level. These results suggested that NSPCK can influence the gut microbiome environment by modulating and altering the abundance and diversity of various bacterial populations.

3.7. Spearman correlation analysis of gut microbiota and SCFAs

To clarify the relationship between gut bacterial changes and obesity-related traits, the Spearman correlation coefficient between

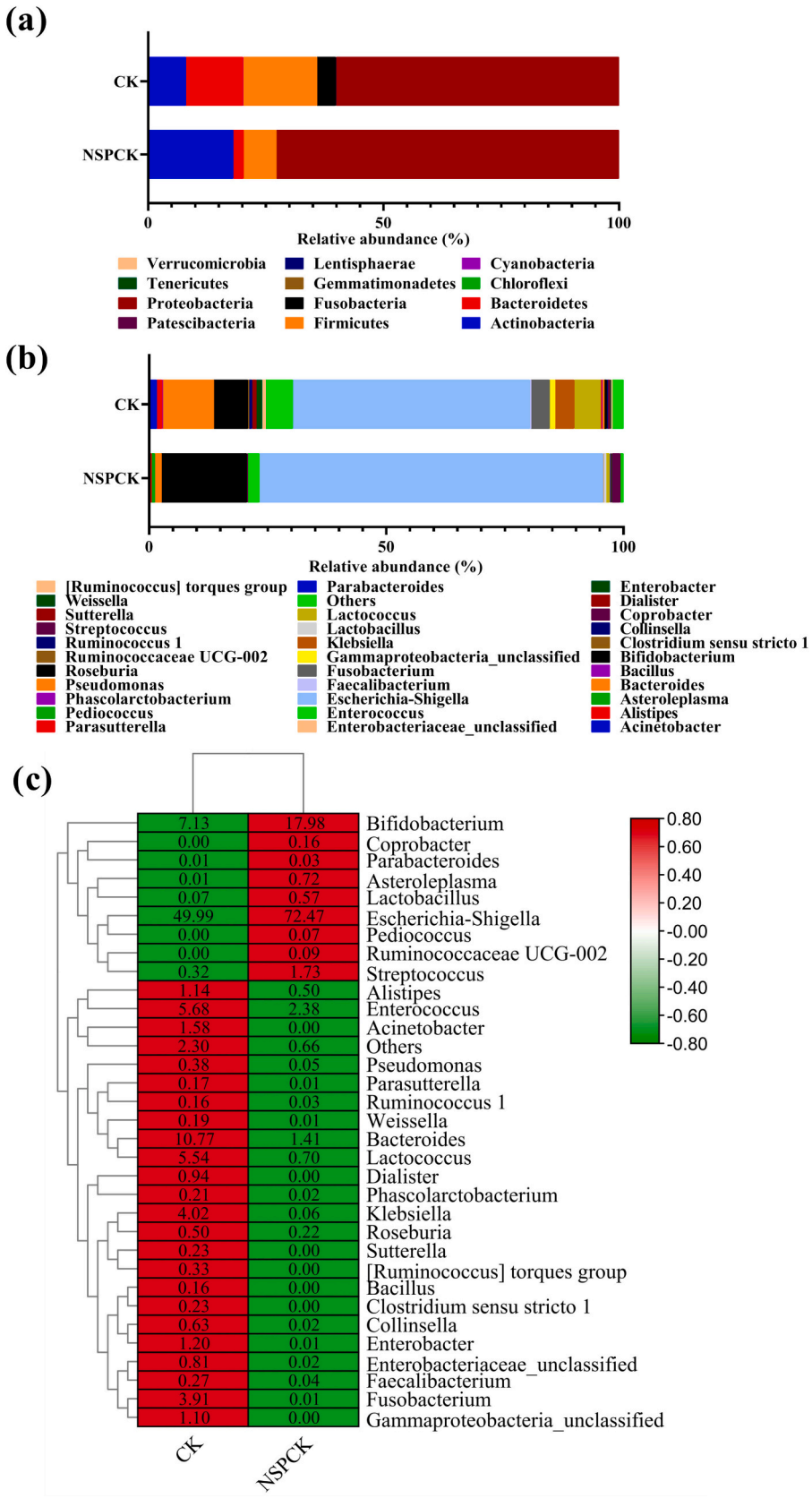

Fig. 4. Effects of CK and NSPCK on gut microbiota. (a) Phylum level; (b) Genus level; (c) Heatmap analysis of the relative abundance of bacterial community at the genus level.

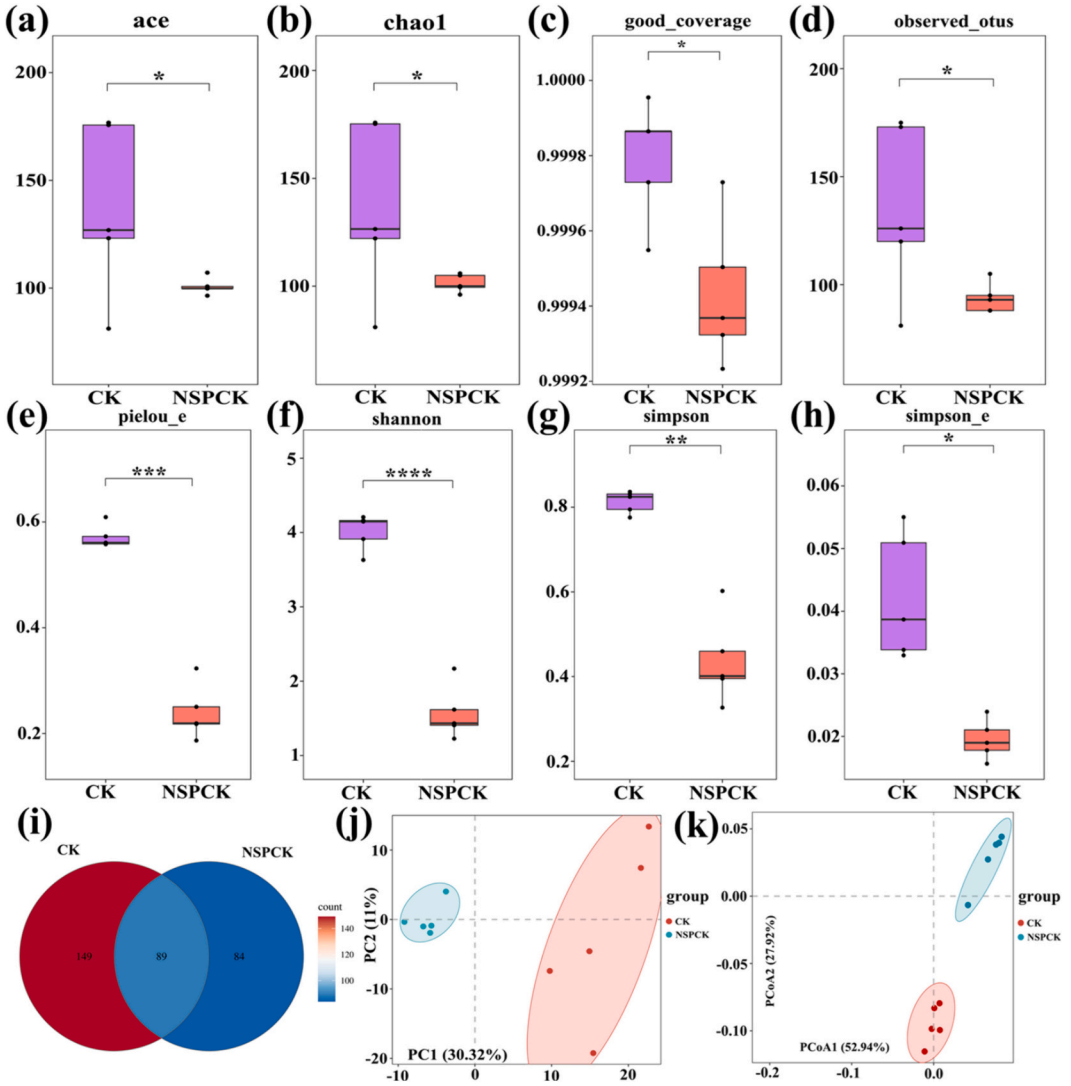

Fig. 5. Analysis of microbial Alpha diversity and Beta diversity. Alpha-diversity was presented by a box plot of the ace (a), Chao1 (b), goods_coverage (c), observed_otus (d), pielou_e (e), shannon (f), simpson (g), and simpson_e (h); Beta-diversity was presented by Venn display (i), PCA (j), and PCoA (k). Data are presented as mean ± SEM. *$p < 0.05$, **$p < 0.01$, ***$p < 0.001$, ****$p < 0.0001$.

SCFAs and gut microbiota was calculated. A diverse array of changes in gut bacterial populations were positively or negatively correlated with variations in the synthesis of gut metabolites (Fig. 6c). The abundance of some populations such as *Bacillus*, *Collinsella*, and *Lactobacillus* was positively correlated with SCFAs, while that of some other populations such as *Bifidobacterium*, *Enterobacter*, and *Lactococcus* showed negative correlations with SCFAs. The content of acetic acid was the highest, and its correlation results with bacterial populations were similar the those of total SCFAs. The abundance of some populations such as *Asteroleplasma*, *Bacillus*, and *Enterococcus* were positively correlated with propionic acid, while that of *Collinsella*, *Coprobacter* and *Dialister* showed negative correlations with propionic acid. The abundance of some populations such as *Coprobacter*, *Fusobacterium*, and *Klebsiella* was positively correlated with i-butyric acid, and that of some populations such as *Bacillus* and *Clostridium sensu stricto 1* was negatively correlated with i-butyric acid. The correlation results of n-butyric acid and n/i-valeric acid were similar to those of propionic acid, while n/i-hexanoic acid showed similar correlation results to i-butyric acid.

3.8. Differences in gut microbiome function

The KEGG functional profiles of the gut microbiota were assessed through PICRUSt analysis. Statistically significant differences ($p < 0.05$) in the KEGG metabolic pathway were observed between the NSPCK group and the CK group. As depicted in Fig. 6d, thirteen metabolic pathways, such as xenobiotics biodegradation and metabolism, lipid metabolism, and glycan biosynthesis and metabolism, exhibited significant enrichment ($p < 0.05$) in the NSPCK group. Among these, the metabolism of cofactors and vitamins stood out as the most enriched metabolic pathway across all groups, followed by infectious diseases and endocrine system, which showed significantly higher enrichment in the NSPCK group than in the CK group. However, converse results were obtained for the enrichment in metabolism of other amino acids and lipid metabolism.

4. Conclusion

This study aims to evaluate the changes in the properties of NSPCK after simulated *in vitro* gastrointestinal digestion and fermentation, as well as their impact on specific microorganisms implicated in human health. Additionally, the study also assessed the effects of NSPCK on blood lipid level and colon tissue in a mouse model. We revealed that NSPCK undergoes partial degradation during *in vitro* digestion, with some changes in its antioxidant and hypoglycemic activities but little

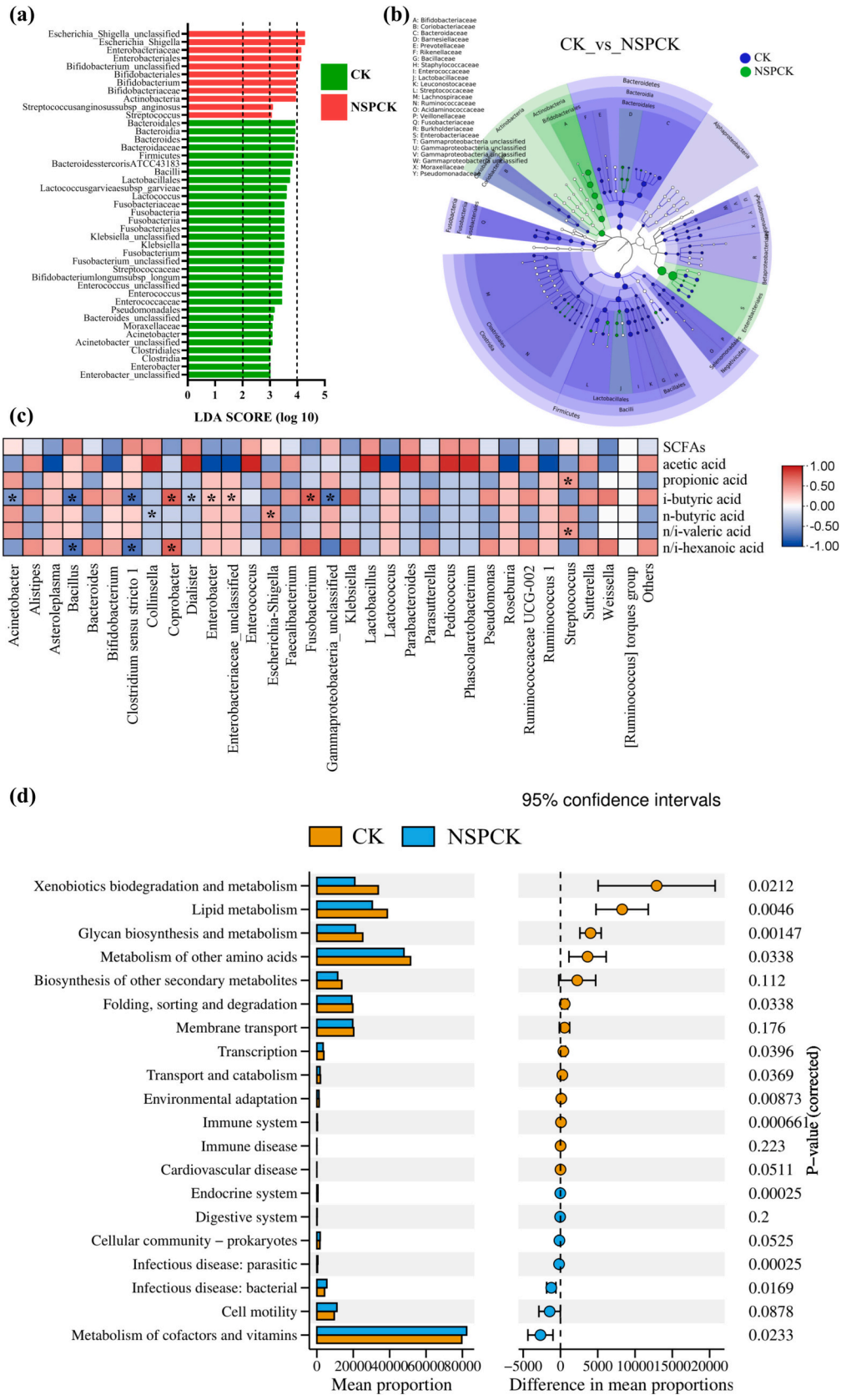

Fig. 6. LDA (a) and Lefse (b) analysis of microbiota. Spearman correlation analysis of gut microbiota and SCFAs (c). Spearman's correlation analysis was calculated between 32 identified bacterial genera and obesity traits. Prediction of differences in microbial function at KEGG pathway level (d). *$p < 0.05$.

variation in its efficacy and structure. Intervention with NSPCK could significantly reduce and lipid levels, as well as affect the muscularis thickness in mice fed a standard diet. Analysis of the changes in gut microbiota composition after fermentation indicated that supplementation with NSPCK can significantly elevate the SCFAs level, thereby bringing about a favorable effect on metabolic processes of the gut microbiota. Assessment on the effect of NSPCK on the gut microbiota composition further suggested its capability to significantly reshape the gut environment and enhance the abundance of beneficial bacteria such as *Bifidobacterium* and *Lactobacillus*, while concurrently reduce the level of harmful bacteria such as *Fusobacteria* and *Enterococcus*, ultimately increasing the diversity and richness of the gut microbial community. Collectively, NSPCK demonstrates considerable potential in modulating the gut microbiota, and our findings indicate that NSPCK can confer numerous health benefits to consumers as a functional prebiotic food.

Funding

This project is supported by the National Natural Science Foundation of China (U22A20545).

CRediT authorship contribution statement

Fei Peng: Writing – review & editing, Writing – original draft, Visualization, Supervision, Methodology. **Zuoqing Yu:** Writing – review & editing, Writing – original draft, Software, Methodology, Data curation. **Kui Niu:** Visualization, Investigation, Data curation. **Bin Du:** Visualization, Investigation, Data curation. **Shujun Wang:** Visualization, Supervision. **Yuedong Yang:** Visualization, Supervision.

Declaration of competing interest

The authors declare that they have no known competing financial interests or personal relationships that could have appeared to influence the work reported in this paper.

Data availability

Data will be made available on request.

Acknowledgements

The authors gratefully acknowledge Analysis and Testing Centre of Hebei Normal University of Science and Technology for providing testing equipment.

References

Al-Lahham, S. A. H., Roelofsen, H., Priebe, M., Weening, D., Dijkstra, M., Hoek, A., … Vonk, R. J. (2010). Regulation of adipokine production in human adipose tissue by propionic acid. *European Journal of Clinical Investigation, 40*(5), 401–407.

Chen, J., Chen, Y., Hu, J., He, C., Peng, X., Li, Z., Wang, Y., Zhu, M., & Xiao, Y. (2023). Solid-state fermentation with Rhizopus oryzae HC-1 improves the metabolites profiling, antioxidant activity and gut microbiota modulation effect of soybeans. *LWT, 187*, Article 115253.

Chen, P., Lei, S., Tong, M., Chang, Q., Zheng, B., Zhang, Y., & Zeng, H. (2022). Effect of polysaccharide fractions from Fortunella margarita on the fecal microbiota of mice and SCFA production in vitro. *Food Science and Human Wellness, 11*(1), 97–108.

Chen, P., Liu, L., Cheng, Z., Zhang, Y., Zheng, B., Hu, X., … Wellness, H. (2023). Structure elucidation and in vitro rat intestinal fermentation properties of a novel sulfated glucogalactan from Porphyra haitanensis. *Food Science and Human Wellness, 12*(2), 596–606.

Chen, S., Luan, L., Zhang, Y., Liu, F., Ye, X., & Hou, Z. (2023). A comparison study on polysaccharides extracted from Rosa sterilis S.D.Shi using different methods: Structural and in vitro fermentation characterizations. *Food Chemistry: X, 17*, Article 100533.

Ding, Q. (2021). *The mechanism of polysaccharides from Ganoderma atrum on type 2 diabetic rats through gut microbiota*. Nanchang University.

Egger, L., Ménard, O., Baumann, C., Duerr, D., Schlegel, P., Stoll, P., Vergères, G., Dupont, D., & Portmann, R. (2019). Digestion of milk proteins: Comparing static and dynamic in vitro digestion systems with in vivo data. *Food research international (Ottawa, Ont.), 118*, 32–39.

El-Far, M., Durand, M., Turcotte, I., Larouche-Anctil, E., Sylla, M., Zaidan, S., … i. i.. (2021). Upregulated IL-32 expression and reduced gut short chain fatty acid caproic acid in people living with HIV with subclinical atherosclerosis. *Frontiers in Immunology, 12*, Article 664371.

Esteves, B., Velez Marques, A., Domingos, I., & Pereira, H. (2013). Chemical changes of heat treated pine and eucalypt wood monitored by FTIR *Maderas. Ciencia y Tecnología, 15*, 245–258.

Ferreira-Lazarte, A., Moreno, F. J., Cueva, C., Gil-Sánchez, I., & Villamiel, M. (2019). Behaviour of citrus pectin during its gastrointestinal digestion and fermentation in a dynamic simulator (simgi®). *Carbohydrate Polymers, 207*, 382–390.

Ge, Q., Hou, C., Rao, X., Zhang, A., Xiao, G., Wang, L., Jin, K., Sun, P., & Chen, L. (2024). In vitro fermentation characteristics of polysaccharides from coix seed and its effects on the gut microbiota. *International Journal of Biological Macromolecules, 262*, Article 129994.

Geng, X., Guo, D., Bau, T., Lei, J., Xu, L., Cheng, Y., Feng, C., Meng, J., & Chang, M. (2023). Effects of in vitro digestion and fecal fermentation on physico-chemical properties and metabolic behavior of polysaccharides from Clitocybe squamulosa. *Food Chemistry: X, 18*, Article 100644.

Golpour, F., Abbasi-Alaei, M., Babaei, F., Mirzababaei, M., Parvardeh, S., Mohammadi, G., & Nassiri-Asl, M. (2023). Short chain fatty acids, a possible treatment option for autoimmune diseases. *Biomedicine & Pharmacotherapy, 163*, Article 114763.

Harris, S., Powers, S., Monteagudo-Mera, A., Kosik, O., Lovegrove, A., Shewry, P., & Charalampopoulos, D. (2020). Determination of the prebiotic activity of wheat arabinogalactan peptide (AGP) using batch culture fermentation. *European Journal of Nutrition, 59*(1), 297–307.

Hashemifesharaki, R., Xanthakis, E., Altintas, Z., Guo, Y., & Gharibzahedi, S. M. T. (2020). Microwave-assisted extraction of polysaccharides from the marshmallow roots: Optimization, purification, structure, and bioactivity. *Carbohydrate Polymers, 240*, Article 116301.

Henneke, L., Schlicht, K., Andreani, N. A., Hollstein, T., Demetrowitsch, T., Knappe, C., … Laudes, M. (2022). A dietary carbohydrate – Gut Parasutterella – Human fatty acid biosynthesis metabolic axis in obesity and type 2 diabetes. *Gut Microbes, 14*(1), 2057778.

Jia, F., Liu, X., Gong, Z., Cui, W., Wang, Y., Wang, W. J. F. S., & Nutrition.. (2020). Extraction, modification, and property characterization of dietary fiber from *Agrocybe cylindracea*. *Food Science & Nutrition, 8*(11), 6131–6143.

Jonathan, M. C., van den Borne, J. J. G. C., van Wiechen, P., Souza da Silva, C., Schols, H. A., & Gruppen, H. (2012). In vitro fermentation of 12 dietary fibres by faecal inoculum from pigs and humans. *Food Chemistry, 133*(3), 889–897.

Juśkiewicz, J., Ognik, K., Fotschki, J., Napiórkowska, D., Cholewińska, E., Grzelak-Błaszczyk, K., Krauze, M., & Fotschki, B. (2023). The effects of dietary chromium supplementation along with discontinuing a high-fat diet on the microbial enzymatic activity and the production of SCFAs in the Faeces of rats. *Nutrients, 15*(18), 3962.

Kappel, B. A., De Angelis, L., Puetz, A., Ballanti, M., Menghini, R., Marx, N., & Federici, M. J. P. R. (2023). Antibiotic-induced gut microbiota depletion exacerbates host hypercholesterolemia. *Pharmacological Research, 187*, Article 106570.

Lavelle, A., & Sokol, H. (2020). Gut microbiota-derived metabolites as key actors in inflammatory bowel disease. *Nature Reviews Gastroenterology & Hepatology, 17*(4), 223–237.

Li, R., Sharma, A. K., Zhu, J., Zheng, B., Xiao, G., & Chen, L. (2022). Nutritional biology of chestnuts: A perspective review. *Food Chemistry, 395*, Article 133575.

Li, X., Zhou, P., Luo, Z., Feng, R., & Wang, L. (2022). Hohenbuehelia serotina polysaccharides self-assembled nanoparticles for delivery of quercetin and their anti-proliferative activities during gastrointestinal digestion in vitro. *International Journal of Biological Macromolecules, 203*, 244–255.

Lu, H., You, Y., Zhou, X., He, Q., Wang, M., Chen, L., … Lou, L. (2021). Citrus reticulatae pericarpium Extract Decreases the Susceptibility to HFD-Induced Glycolipid Metabolism Disorder in Mice Exposed to Azithromycin in Early Life. *Frontiers in Immunology*, 12.

Luo, Q., Li, X., Li, H., Kong, K., Li, C., Fang, Z., Hu, B., Wang, C., Chen, S., Wu, W., Li, X., Liu, Y., & Zeng, Z. (2023). Effect of in vitro simulated digestion and fecal fermentation on boletus auripes polysaccharide characteristics and intestinal flora. *International Journal of Biological Macromolecules, 249*, Article 126461.

Rajput, A., Chauhan, S. M., Mohite, O. S., Hyun, J. C., Ardalani, O., Jahn, L. J., … Palsson, B. O. (2023). Pangenome analysis reveals the genetic basis for taxonomic classification of the Lactobacillaceae family. *Food Microbiology, 115*, Article 104334.

Riyadi, P. H., Romadhon Wijayanti, I., Arifin, M. H., Sunaya, N., & Gulzar, S. (2023). Optimization of threadfin bream (Nemipterus sp.) protein hydrolysate using response surface methodology analysis. *IOP Conference Series: Earth and Environmental Science, 1224*(1), Article 012035.

Salvador, V., Cherbut, C., Barry, J.-L., Bertrand, D., Bonnet, C., & Delort-Laval, J. (1993). Sugar composition of dietary fibre and short-chain fatty acid production during in vitro fermentation by human bacteria. *British Journal of Nutrition, 70*(1), 189–197.

Song, S., Qiu, Z., Sun-Waterhouse, D., Bai, X., Xiang, L., Zheng, Z., & Qiao, X. (2023). Garlic polysaccharide-Cr (III) complexes with enhanced in vitro and in vivo hypoglycemic activities. *International Journal of Biological Macromolecules, 237*, Article 124178.

Sun, C., Wu, X., Chen, X., Li, X., Zheng, Z., & Jiang, S. (2020). Production and characterization of okara dietary fiber produced by fermentation with Monascus anka. *Food Chemistry, 316*, Article 126243.

Uthumporn, U., Nadiah, I., Izzuddin, I., Cheng, L., & Aida, H. J. S. M. (2017). Physicochemical characteristics of non-starch polysaccharides extracted from cassava tubers. *Sains Malaysiana, 46*(2), 223–229.

Wang, H., Gou, W., Su, C., Du, W., Zhang, J., Miao, Z., Xiao, C., Jiang, Z., Wang, Z., Fu, Y., Jia, X., Ouyang, Y., Jiang, H., Huang, F., Li, L., Zhang, B., & Zheng, J.-S. (2022). Association of gut microbiota with glycaemic traits and incident type 2 diabetes, and modulation by habitual diet: A population-based longitudinal cohort study in Chinese adults. *Diabetologia, 65*(7), 1145–1156.

Wang, L., Xu, H., Yuan, F., Fan, R., & Gao, Y. (2015). Preparation and physicochemical properties of soluble dietary fiber from orange peel assisted by steam explosion and dilute acid soaking. *Food Chemistry, 185*, 90–98.

Watanabe, Y., Nagai, F., & Morotomi, M. (2012). Characterization of Phascolarctobacterium succinatutens sp. nov., an Asaccharolytic, succinate-utilizing bacterium isolated from human feces. *Applied and Environmental Microbiology, 78*(2), 511–518.

Wijesekara, T., Huang, R., Wong, I. N., & Xu, B. (2024). Insights into immunoregulatory effects of bioactive polysaccharides derived from seaweeds through gut microbiota. *Food Bioscience, 58*, Article 103800.

Xie, F. Y., Li, F. F., Zhang, S., Bi, W. W., Zhang, X. L., & Zhang, X. N. (2018). Analysis of acylation modification of black Rice anthocyanins using Fourier transform infrared spectroscopy (FTIR). *Spectroscopy and Spectral Analysis, 38*(8), 2386–2389.

Xue, H., Liang, B., Wang, Y., Gao, H., Fang, S., Xie, K., & Tan, J. (2024). The regulatory effect of polysaccharides on the gut microbiota and their effect on human health: A review. *International Journal of Biological Macromolecules, 270*, Article 132170.

Yang, J. X., Liu, C. W., Wu, F. W., Zhu, L., & Liang, G.-W. (2024). Molecular characterization and biofilm formation ability of Enterococcus faecium and Enterococcus faecalis bloodstream isolates from a Chinese tertiary hospital in Beijing. *International Microbiology, 27*(3), 929–939.

Zhang, W., Zeng, G., Pan, Y., Chen, W., Huang, W., Chen, H., & Li, Y. J. C. P. (2017). Properties of soluble dietary fiber-polysaccharide from papaya peel obtained through alkaline or ultrasound-assisted alkaline extraction. *Carbohydrate Polymers, 172*, 102–112.

Zhang, Y., Qi, C., Li, X., Geng, M., Lan, H., Wei, Y., Luo, D., Bai, Z., Guo, J., & Han, S. (2024). Research on the effects of intestinal FXR agonists and antibiotics on the regulation of red kidney bean polysaccharides in the liver metabolism in mice with type 2 diabetes. *eFood, 5*(3), Article e159.